

*Citation for published version:*

Sayers, C, Hedayat, H, Ceraso, A, Museur, F, Cattelan, M, Hart, L, Farrar, L, Dal Conte, S, Cerullo, G, Dallera, C, Da Como, E & Carpine, E 2020, 'Coherent phonons and the interplay between charge density wave and Mott phases in 1T-TaSe<sub>2</sub>', *Physical Review B*, vol. 102, no. 16, 161105(R).  
<https://doi.org/10.1103/PhysRevB.102.161105>

*DOI:*

[10.1103/PhysRevB.102.161105](https://doi.org/10.1103/PhysRevB.102.161105)

*Publication date:*

2020

*Document Version*

Peer reviewed version

[Link to publication](#)

(C) American Physical Society, 2020.

**University of Bath**

## **Alternative formats**

If you require this document in an alternative format, please contact:  
[openaccess@bath.ac.uk](mailto:openaccess@bath.ac.uk)

### **General rights**

Copyright and moral rights for the publications made accessible in the public portal are retained by the authors and/or other copyright owners and it is a condition of accessing publications that users recognise and abide by the legal requirements associated with these rights.

### **Take down policy**

If you believe that this document breaches copyright please contact us providing details, and we will remove access to the work immediately and investigate your claim.

# Coherent phonons and the interplay between charge density wave and Mott phases in $1T$ -TaSe<sub>2</sub>

C. J. Sayers,<sup>1,2,\*</sup> H. Hedayat,<sup>1,3</sup> A. Ceraso,<sup>1</sup> F. Musser,<sup>4</sup> M. Cattelan,<sup>5</sup> L. S. Hart,<sup>2</sup>  
L. S. Farrar,<sup>2</sup> S. Dal Conte,<sup>1</sup> G. Cerullo,<sup>1</sup> C. Dallera,<sup>1</sup> E. Da Como,<sup>2</sup> and E. Carpene<sup>3</sup>

<sup>1</sup>*Dipartimento di Fisica, Politecnico di Milano, 20133 Milano, Italy*

<sup>2</sup>*Centre for Nanoscience and Nanotechnology, Department of Physics, University of Bath, Bath, BA2 7AY, UK*

<sup>3</sup>*IFN-CNR, Dipartimento di Fisica, Politecnico di Milano, 20133 Milano, Italy*

<sup>4</sup>*Université de Lyon, ENS de Lyon, Université Claude Bernard,*

*CNRS, Laboratoire de Physique, F-69342 Lyon, France*

<sup>5</sup>*School of Chemistry, University of Bristol, Cantocks Close, Bristol BS8 1TS, UK*

$1T$ -TaSe<sub>2</sub> is host to coexisting strongly-correlated phases including charge density waves (CDWs) and an unusual Mott transition at low temperature. Here, we investigate coherent phonon oscillations in  $1T$ -TaSe<sub>2</sub> using a combination of time- and angle-resolved photoemission spectroscopy (TR-ARPES) and time-resolved reflectivity (TRR). Perturbation by a femtosecond laser pulse triggers a modulation of the valence band binding energy at the  $\bar{\Gamma}$ -point, related to the Mott gap, that is consistent with the in-plane CDW amplitude mode frequency. By contrast, TRR measurements show a modulation of the differential reflectivity comprised of multiple frequencies belonging to the distorted CDW lattice modes. Comparison of the temperature dependence of coherent and spontaneous phonons across the CDW transition shows that the amplitude mode intensity is more easily suppressed during perturbation of the CDW state by the optical excitation compared to other modes. Our results clearly identify the relationship of the in-plane CDW amplitude mode with the Mott phase in  $1T$ -TaSe<sub>2</sub> and highlight the importance of lattice degrees of freedom.

## I. INTRODUCTION

Understanding the delicate interplay between co-operating or competing phases of matter in quantum materials is an ongoing goal of fundamental research [1–3]. Driving these systems out of equilibrium using an intense femtosecond laser pulse offers the possibility to transiently suppress forms of electronic and lattice order and monitor their recovery in real time [4]. The characteristic dynamics of these processes allows a classification of materials in the time-domain [5], and has been used to disentangle the underlying mechanisms of complex phases found in cuprate superconductors [6] and exciton-lattice driven CDW systems [7], or to unlock normally hidden states of matter [8].

An ideal platform to investigate these phenomena are the trigonal ( $1T$ ) tantalum-based transition metal dichalcogenides (TMDs), MX<sub>2</sub> (M = Ta, X = S/Se) which are host to a whole range of strongly-correlated behaviour including charge density waves (CDWs) [9], Mott physics [10], possible quantum spin liquid states [11], and superconductivity [12, 13].

Tantalum disulphide ( $1T$ -TaS<sub>2</sub>) has been studied extensively using time-resolved techniques [14–20], motivated mostly by its rich phase diagram. It exhibits multiple CDW transitions including an incommensurate (550 K), nearly-commensurate (350 K), and commensurate (180 K) phase [9] that occurs concomitantly with a metal-insulator transition, commonly associated with a Mott phase [21]. However, an alternative explanation has

recently been proposed based on the three-dimensional stacking order of the CDW and hybridization of atomic orbitals [22–24]. Thus, important questions surrounding the nature of the metal-insulator transition and its relationship with the CDW remain.

Tantalum diselenide ( $1T$ -TaSe<sub>2</sub>) has received comparatively far less attention, although it was recently suggested to be the more suitable compound to investigate the relationship between the CDW and Mott phases because of the well-separated transition temperatures, larger electronic gap, and reduced complexity due to the absence of the nearly-commensurate phase (NCCDW) [19].

$1T$ -TaSe<sub>2</sub> undergoes a first-order transition from an incommensurate (ICCDW) to commensurate (CCDW) charge density wave at  $T_{\text{CDW}} = 473$  K [25]. It is accompanied by an in-plane  $\sqrt{13}a_0 \times \sqrt{13}a_0$  periodic lattice distortion (PLD) which is rotated by  $\sim 13^\circ$  with respect to the original unit cell, and forms a 13-atom superlattice comprised of Ta clusters in the so-called “star-of-David” configuration [9].

In addition to the well known CDW, a Mott transition occurs at  $\sim 260$  K evidenced by the opening of a gap,  $\Delta_{\text{Mott}} \approx 250$  meV below the Fermi level,  $E_F$  observed by ARPES [10] and STM [26]. The CDW has been suggested to be a precursor to the Mott phase, since it modifies the band structure resulting in a narrow half-filled band at  $E_F$ . As the temperature is reduced, the increasing CDW amplitude causes a narrowing of the band width ( $W$ ), related to the in-plane electron hopping between the adjacent star-of-David clusters in the CDW lattice [27, 28]. Electrons will become localized when the band width ( $W$ ) decreases below a critical value and the Mott criterion,  $U/W \geq 1$  is reached, where  $U$  is the on-

\* Corresponding author: [charles.sayers@polimi.it](mailto:charles.sayers@polimi.it)

74 site electron-electron Coulomb repulsion. The result of  
75 this localization is a transition to an insulating state and  
76 formation of a gap,  $\Delta_{\text{Mott}}$  [10, 26].

77 Time- and angle-resolved photoemission spectroscopy  
78 (TR-ARPES) is a powerful tool which allows direct visu-  
79 alization of the electronic band structure following per-  
80 turbation with a laser pulse. In strongly-correlated sys-  
81 tems, it can be used to monitor the collapse and recovery  
82 of electronic order in real-time by probing energy gaps,  $\Delta$   
83 related to the order parameter [5–7]. Recent TR-ARPES  
84 studies of 1T-TaSe<sub>2</sub> using high-harmonics ( $h\nu \approx 22$  eV)  
85 have focused predominantly on gap suppression dynamics  
86 on short timescales [19] or the room temperature (CDW)  
87 phase only [29], and thus the Mott phase dynamics re-  
88 main relatively unexplored.

89 Here, we report on electron and phonon dynamics of  
90 1T-TaSe<sub>2</sub> at low temperature (77 K) where the CDW  
91 and Mott phases co-exist. Using TR-ARPES with  $h\nu =$   
92 6 eV photon energy, we track the temporal evolution of  
93 the valence band binding energy related to  $\Delta_{\text{Mott}}$  at the  
94  $\bar{\Gamma}$ -point over several picoseconds. We find that it exhibits  
95 strong, long-lasting oscillations with a single frequency  
96 related to the in-plane CDW amplitude mode ( $\sim 2.2$   
97 THz at 77 K). Using complementary time-resolved re-  
98 flectivity (TRR) measurements, we instead find multiple  
99 phonon frequencies related to the PLD ( $\sim 1.8, 2.2$  and  
100 2.9 THz). Therefore, aided by the momentum-selectivity  
101 of TR-ARPES, our results reveal that the gap,  $\Delta_{\text{Mott}}$  is  
102 linked preferentially to the amplitude mode of the CDW.  
103 By investigating the temperature-dependence of coher-  
104 ent phonons, we find that the amplitude mode deviates  
105 significantly from first-order behaviour, whilst the other  
106 modes are robust up to  $T_{\text{CDW}}$ , highlighting further the  
107 nature of this mode and its importance to electronic or-  
108 der in this material.

## 109 II. METHODS

110 TR-ARPES experiments were performed using visible  
111 ( $\sim 1.8$  eV, 30 fs) pump and deep-ultraviolet ( $\sim 6.0$  eV, 80  
112 fs) probe pulses generated by a series of nonlinear optical  
113 processes from the output of an Yb-based laser (Pharos,  
114 Light Conversion) operating at 80 kHz repetition rate,  
115 as described in Ref. [30]. The overall time- and energy-  
116 resolution of this configuration were approximately 80  
117 fs and 45 meV, respectively. TRR was performed using  
118 a setup based on a Ti:sapphire laser (Coherent Li-  
119 bra) which drives two non-collinear parametric amplifiers  
120 (NOPAs) serving as pump and probe beams [31]. The  
121 amplified pulses are characterized by a broad spectrum  
122 of (1.8 - 2.4) eV and compressed to  $\leq 20$  fs duration us-  
123 ing chirped mirrors. Steady-state ARPES measurements  
124 were performed at the Bristol NanoESCA facility using  
125 He-I $\alpha$  radiation ( $h\nu = 21.2$  eV), with  $\sim 50$  meV energy  
126 resolution at 40 K. Further experimental details relat-  
127 ing to crystal growth methods, electrical transport mea-  
128 surements, and Raman spectroscopy are provided in the

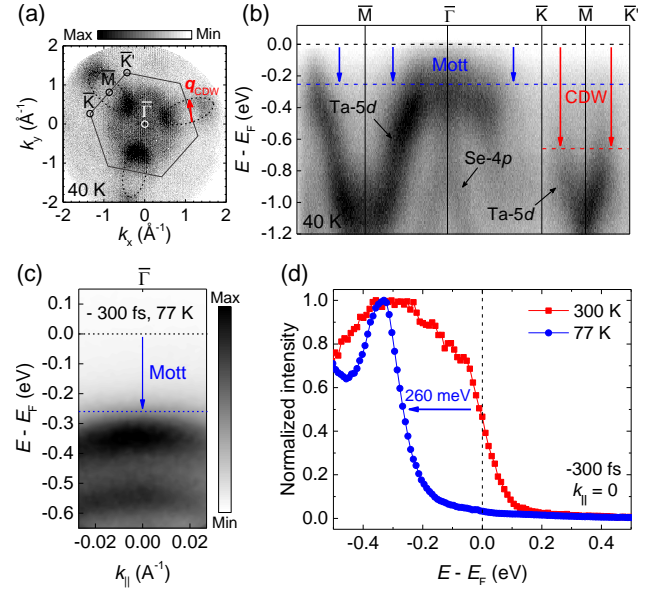


FIG. 1. Electronic order in 1T-TaSe<sub>2</sub>. (a) Full-wavevector ARPES ( $h\nu = 21.2$  eV) image of the electronic structure,  $E - E_F = -0.5$  eV at 40 K with projected high-symmetry points of the hexagonal Brillouin zone (BZ) labelled. The red arrow is the expected CDW vector,  $\mathbf{q}_{\text{CDW}}$ . (b) Band dispersions through the BZ. The vertical arrows highlight the lowering of occupied states due to the CDW (red) and Mott (blue) transitions. (c) TR-ARPES ( $h\nu = 6$  eV) map at 77 K. (d) Comparison of EDCs extracted from the  $\bar{\Gamma}$ -point ( $k_{\parallel} = 0$ ) at 300 K and 77 K. The arrow shows the band edge shift as a result of the Mott transition.

Supplemental Material (Ref. [32]).

## 130 III. RESULTS AND DISCUSSION

131 First we discuss the electronic structure of 1T-  
132 TaSe<sub>2</sub> and the effects of CDW and Mott transitions.  
133 Fig. 1(a) shows a full-wavevector ARPES image at  $E -$   
134  $E_F = -0.5$  eV where all the main features are visible. Cen-  
135 tred around the  $\bar{M}$ -points on the BZ boundary are the  
136 elliptical Ta-5d electron pockets, and at the BZ centre  
137 ( $\bar{\Gamma}$ -point) is the Se-4p pocket, in agreement with previ-  
138 ous ARPES measurements [33, 34]. The CDW involves  
139 finite portions of the Ta-5d electron pockets which are  
140 linked by the wavevector,  $\mathbf{q}_{\text{CDW}}$  in the  $\bar{K}$ - $\bar{M}$ - $\bar{K}$  direction  
141 where the Fermi surface could be prone to nesting [9, 19],  
142 although the importance of such electronic instabilities is  
143 still debated [33, 35]. Indeed, there is a clear loss of inten-  
144 sity on the parallel arms of these pockets in Fig. 1(a), and  
145 dispersion along the  $\bar{K}$ - $\bar{M}$ - $\bar{K}$  direction in Fig. 1(b) shows  
146 the band edge is found significantly below  $E_F$  as a result  
147 of the CDW gap,  $\Delta_{\text{CDW}}$ . Dispersion along the  $\bar{M}$ - $\bar{\Gamma}$  di-  
148 rection in Fig. 1(b) shows a valence band comprised of  
149 broad Ta-5d states, and steeply dispersing Se-4p states,  
150 which are known to extend to  $E_F$  at room temperature  
151 [10]. At 40 K, all bands near  $E_F$  have been lowered by

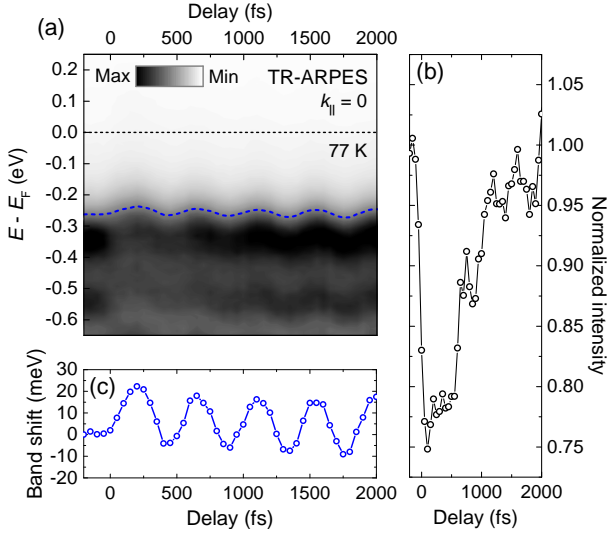


FIG. 2. Valence band dynamics in the CDW-Mott phase. (a) TR-ARPES spectra at the  $\bar{\Gamma}$ -point (77 K) using 1.10 mJ cm $^{-2}$  pump fluence. (b) Normalized valence band intensity, extracted from the maximum near  $E - E_F \approx -0.35$  eV. (c) Valence band shift extracted from a constant intensity contour in panel (a), indicated by the blue dashed line.

~250 meV due to a gap,  $\Delta_{\text{Mott}}$  which extends across all  $k$ -space, and thus the entire Fermi surface is removed [32].

Shown in Fig. 1(c) are TR-ARPES spectra of 1T-TaSe $_2$  at 77 K near the  $\bar{\Gamma}$ -point before pump arrival (-300 fs). The dispersion is approximately along the  $\bar{\Gamma}$ - $\bar{M}$  direction based on low energy electron diffraction (LEED) [32]. Fig. 1(c) clearly shows the band edge is situated below  $E_F$  due to the opening of a gap. A comparison of the energy distribution curves (EDCs) in Fig. 1(d) extracted at  $\bar{\Gamma}$  ( $k_{\parallel} = 0$ ) shows a lowering of the band edge by  $\sim 260$  meV between 300 K and 77 K, which is in very close agreement with previous reports of the Mott transition in 1T-TaSe $_2$  [10] and the ARPES measurements in Fig. 1(b).

We note that such a substantial modification of the Fermi surface, as seen in Fig 1(c) and (d), typically indicates the development of an insulating state, which would be expected to be observed by electrical transport [36]. However, our resistance measurements show metallic behaviour to 4 K [32]. These contrasting results between surface probe (ARPES) and bulk probe (transport) have previously provided support for the hypothesis that the Mott transition in 1T-TaSe $_2$  is only a surface effect [10]. However, we emphasize that for TR-ARPES at  $h\nu = 6$  eV, the inelastic mean free path for electrons is expected to be of the order  $\sim 10$  nm [37] and hence the photoemission signal may represent several layers of 1T-TaSe $_2$  given the  $c$ -axis length of 0.63 nm [25]. Thus, the Mott phase may extend over more than the surface layers.

We now focus on the valence band dynamics in the

coexisting CDW-Mott phase measured by TR-ARPES. Fig. 2(a) shows the valence band at the  $\bar{\Gamma}$ -point after perturbation by the pump pulse. At  $t = 0$ , the optical excitation results in an instantaneous loss of valence band intensity as highlighted in Fig. 2(b), and recovery occurs within  $\sim 2$  ps which is similar to the reported dynamics of 1T-TaS $_2$  in the Mott phase [14]. As is clearly evident by the persisting gap,  $\Delta_{\text{Mott}}$  in Fig. 2(a), we do not observe a collapse of the Mott phase and we also note that 1.10 mJ cm $^{-2}$  pump fluence is not sufficient to melt the CDW [38]. Hence, we confirm that the TR-ARPES experiments were performed in the coexisting CDW-Mott phase.

Fig. 2(c) shows the temporal evolution of the valence band edge position. Most noticeably, the pump triggers strong coherent oscillations which are weakly damped. TR-ARPES data in Fig. 3(a) shows a maximum initial oscillation of approximately  $\pm 20$  meV around the equilibrium position with a large amplitude that persists at 6 ps. Fitting the data with a damped periodic function  $E(t) = A \exp(-t/\tau_d) \sin(2\pi\omega t + \phi)$  yields a frequency,  $\omega \approx (2.19 \pm 0.01)$  THz, which closely matches the intense 72.4 cm $^{-1}$  (2.17 THz)  $A_{1g}$  mode measured by Raman spectroscopy at 77 K [32]. The damping time was found to be  $\tau_d \approx (6.3 \pm 1.0)$  ps. Such long-lived oscillations have also been observed in the Mott phase of 1T-TaS $_2$  [14, 15] and were assigned to the CDW amplitude mode, related to the in-plane breathing mode of the stars-of-David [39]. The result presented here shows a direct modulation of the binding energy of the valence band edge, related to  $\Delta_{\text{Mott}}$ , by the CDW amplitude mode in 1T-TaSe $_2$ . This is consistent with the CDW precursor scenario whereby the CDW amplitude, related to the magnitude of the in-plane PLD, controls the  $U/W$  criterion by the degree of electron hopping between the adjacent stars-of-David [19, 21, 26–28]. By triggering coherent oscillations of the CDW amplitude (breathing) mode, we induce a modulation in the  $U/W$  ratio which manifests in the magnitude of  $\Delta_{\text{Mott}}$ .

To investigate the origin of the coherent phonon oscillations further, we now compare our TR-ARPES results with TRR measurements. Fig. 3(b) shows the temporal evolution of the differential reflectivity,  $\Delta R/R$  of 1T-TaSe $_2$  at 77 K. The  $\Delta R/R$  signal is dominated by strong oscillations that are weakly damped and last up to 20 ps. Interestingly, the oscillations in TRR are comprised of multiple frequencies, in stark contrast to the single-frequency valence band modulation observed by TR-ARPES. This is confirmed by the fast Fourier transform (FFT) of the oscillatory components shown in Fig. 3(c). The FFT of the valence band dynamics shows a single frequency at  $\sim 2.2$  THz, whereas FFT of the TRR signal shows multiple frequencies with greatest amplitude at  $\sim 1.8$ , 2.2 and 2.9 THz, and closely resembles the Raman spectrum presented in Fig. 3(c) and reported previously [40–43]. We note that the  $\sim 1.8$  THz mode cannot be seen in the Raman data as it falls below the cut-off of the spectrometer laser filter. In addition, we note that the 2.2 THz mode appears broader in the



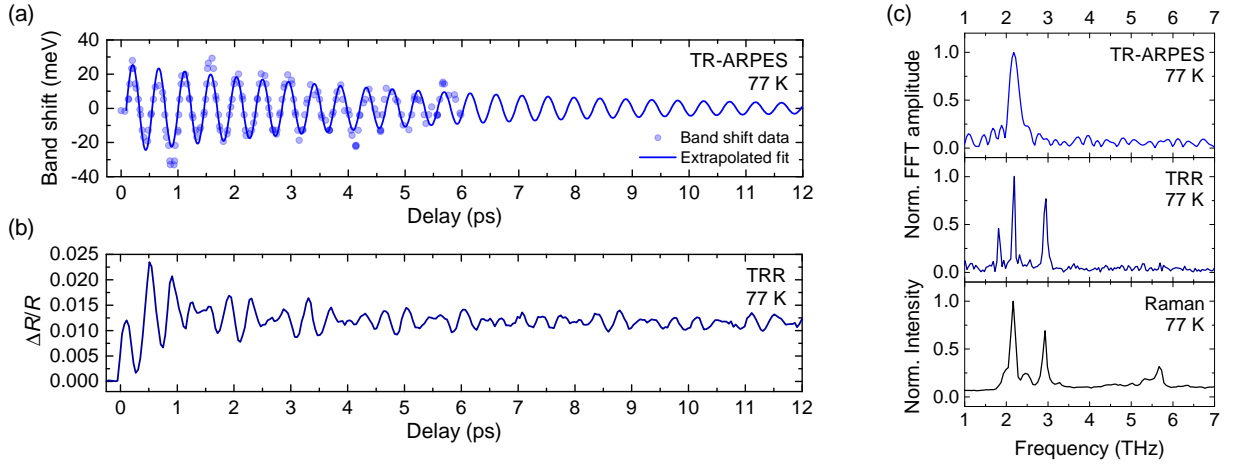


FIG. 3. Coherent phonon oscillations in the CDW-Mott phase. (a) Oscillatory component of the valence band shift measured by TR-ARPES ( $1.16 \text{ mJ cm}^{-2}$ ). (b) Transient reflectivity signal measured by TRR ( $0.11 \text{ mJ cm}^{-2}$ ), where  $\Delta R/R$  is the absolute value of the differential reflectivity. The selected data is for  $1.84 \text{ eV}$  probe photon energy. (c) Normalized fast Fourier transform (FFT) amplitude of the TR-ARPES and TRR oscillatory components, together with a Raman spectrum for comparison.

FFT of the TR-ARPES data because of the shorter sampling interval of the oscillations. Since both TR-ARPES and TRR experiments utilize comparable pump photon energies and pulse durations, it is conceivable that multiple modes are triggered in both cases and relate to the Raman-active  $\Gamma$ -point phonons of the PLD. The energy-momentum selectivity of TR-ARPES directly probes the local electronic structure of the valence band at  $\bar{\Gamma}$  and the interactions there. Hence, the observed modulation of the valence band binding energy ( $\Delta_{\text{Mott}}$ ) with a single frequency belonging to the  $\sim 2.2 \text{ THz}$  CDW amplitude mode, shows that the Mott phase is preferentially linked to that particular mode.

Having established the coherent phonon oscillations of the CDW lattice and the single mode which is linked to the Mott phase, we finally focus on the temperature dependence of these modes, and their behaviour across the CDW transition at  $T_{\text{CDW}}$ . For this, we compare the response of the coherent phonons to optical excitation by TRR, and the spontaneous phonons of the PLD in quasi-equilibrium by Raman spectroscopy. Shown in Fig. 4(a) is a FFT analysis of the  $\Delta R/R$  signal for various sample temperatures in the range (295 - 478) K which are compared to Raman spectra in Fig. 4(b). Similar to the TRR data at 77 K, multiple frequency components are found at 295 K as shown in Fig. 4(a). The peaks in FFT amplitude belong to the two highest intensity modes determined previously [see Fig. 3(c)], although they are found at slightly lower frequencies of  $\sim 2.0$  and  $2.7 \text{ THz}$  because of the higher sample temperature [32]. Fig. 4(a) shows that as the temperature increases in the range (295 - 410) K, the intensity of the  $\sim 2.0 \text{ THz}$  amplitude mode decreases sharply until it becomes absent for  $T \geq 450 \text{ K}$  using  $0.11 \text{ mJ cm}^{-2}$  fluence. Instead, the  $\sim 2.7 \text{ THz}$  mode remains present until heating above the first-order ICCDW-CCDW phase transition at  $T_{\text{CDW}} = 473 \text{ K}$ . By comparison, the Raman data in Fig. 4(b)

shows that all modes remain clearly visible until there is a sudden change in the spectra when heating above  $T_{\text{CDW}}$ . Specifically, we find that all modes merge into a broad background (see Ref. [32]), similar to previous reports [40–43]. The stark difference in the temperature dependence of the mode intensities measured by the two experimental techniques is highlighted by comparing Figs. 4(c) and (d) which show the integrated peak areas in TRR and Raman spectroscopy, respectively. The expected first-order nature of the CDW transition is clear in Fig. 4(d) whereby there is a steep onset at  $T_{\text{CDW}}$  followed by linear temperature dependence, and both the  $\sim 2.0$  and  $2.7 \text{ THz}$  modes exhibit identical behaviour. Instead, Fig. 4(c) shows a dramatic suppression of the  $\sim 2.0 \text{ THz}$  amplitude mode intensity and a deviation from first-order behaviour in TRR, suggestive of a transient photoinduced melting of the CDW amplitude. The  $\sim 2.7 \text{ THz}$  mode however, which is a phonon of the PLD [41], appears to remain robust up to  $T_{\text{CDW}}$ . A complete loss of intensity of the CDW amplitude mode suggests that it has become strongly damped, whereby its lifetime is less than the period of oscillation ( $\approx 0.5 \text{ ps}$ ). Such increased damping could be due to a reduced commensurability between the CDW and the underlying lattice which results in a faster dephasing of the oscillations [15], providing evidence for a suppression of the commensurate state by the optical excitation before the ICCDW-CCDW transition at  $T_{\text{CDW}}$ .

#### IV. CONCLUSION

In summary, an investigation of electron and phonon dynamics in the coexisting CDW-Mott phase of  $1T$ -TaSe<sub>2</sub> using complementary TR-ARPES and TRR techniques clearly shows that the Mott phase is preferentially

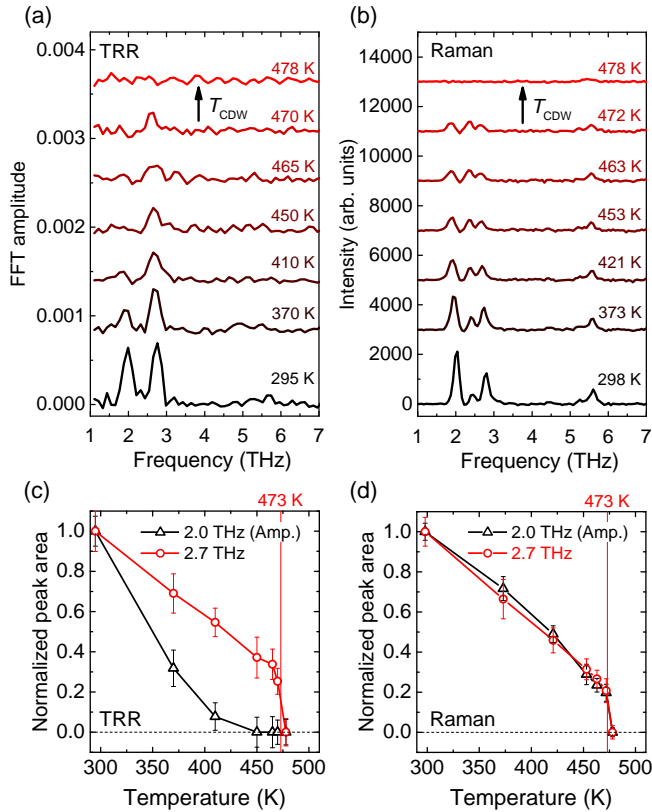


FIG. 4. Temperature dependence of coherent and spontaneous phonons in the CDW phase. (a) Fast Fourier transform (FFT) of the transient reflectivity,  $\Delta R/R$  signal measured by TRR ( $0.11 \text{ mJ cm}^{-2}$ ) at sample temperatures as indicated. The selected data is for  $655 \text{ nm}$  probe wavelength. (b) Raman spectra measured over a similar temperature range as panel (a) for comparison, after subtraction of a fit to the incoherent background signal above  $T_{\text{CDW}}$  ( $478 \text{ K}$ ). All traces are offset for clarity. Panels (c) and (d) show the temperature dependence of the integrated peak area for the  $2.0$  amplitude (Amp.) and  $2.7 \text{ THz}$  modes in the TRR-FFT and Raman spectra respectively.

linked to the in-plane CDW amplitude, since it controls the degree of electron localization between adjacent star-of-David configurations. Our results highlight the role of the CDW and lattice degrees of freedom in stabilizing the Mott phase of  $1T$ -TaSe<sub>2</sub> and further the understanding of the interplay between these coexisting phases.

## ACKNOWLEDGMENTS

The authors acknowledge funding and support from the EPSRC Centre for Doctoral Training in Condensed Matter Physics (CDT-CMP) Grant No. EP/L015544/1 and the Italian PRIN Project No. 2017BZPKSZ. We acknowledge the School of Chemistry at the University of Bristol is for access to the Bristol NanoESCA Facility. Finally, we thank Daniel Wolverson for useful discussions.

- [1] L. J. Li, E. C. T. O'Farrell, K. P. Loh, G. Eda, B. Ozyilmaz, and A. H. C. Neto, Controlling many-body states by the electric field effect in a two-dimensional material, *Nature* **529**, 185 (2016).
- [2] H. H. da Silva Neto, P. Aynajian, A. Frano, R. Comin, E. Schierle, E. Weschke, A. Gyenis, J. Wen, J. Schneeloch, Z. Xu, S. Ono, G. Gu, M. Le Tacon, and Mathieu A. Yazdani, Ubiquitous Interplay Between Charge Ordering and High-Temperature Superconductivity in Cuprates, *Science* **343**, 393 (2014).
- [3] A. Kogar, G. A. de la Pena, Sangjun Lee, Y. Fang, S. X. L. Sun, D. B. Lioi, G. Karapetrov, K. D. Finkelstein, J. P. C. Ruff, P. Abbamonte, and S. Rosenkranz, Observation of a Charge Density Wave Incommensuration Near the Superconducting Dome in  $\text{Cu}_x\text{TiSe}_2$ , *Phys. Rev. Lett.* **118**, 027002 (2017).
- [4] C. Giannetti, M. Capone, D. Fausti, M. Fabrizio, F. Parmigiani and D. Mihailovic, Ultrafast optical spectroscopy of strongly correlated materials and high-temperature superconductors: A non-equilibrium approach, *Adv. Phys.* **65**, 58 (2016).
- [5] S. Hellmann, T. Rohwer, M. Kalläne, K. Hanff, C. Sohrt, A. Stange, A. Carr, M. M. Murnane, H. C. Kapteyn, L. Kipp, M. Bauer, and K. Rossnagel, Time-domain classification of charge-density-wave insulators, *Nat. Commun.* **3**, 1069 (2012).
- [6] F. Boschini, E. H. da Silva Neto, E. Razzoli, M. Zonno, S. Peli, R. P. Day, M. Michiardi, M. Schneider, B. Zwartsenberg, P. Nigge, R. D. Zhong, J. Schneeloch, G. D. Gu, S. Zhdanovich, A. K. Mills, G. Levy, D. J. Jones, C. Giannetti and A. Damascelli, Collapse of superconductivity in cuprates via ultrafast quenching of phase coherence, *Nat. Mater.* **17**, 416 (2018).
- [7] H. Hedayat, C. J. Sayers, D. Bugini, C. Dallera, D. Wolverson, T. Batten, S. Karbassi, S. Friedemann, G. Cerullo, J. van Wezel, S. R. Clark, E. Carpene, and E. Da

- Como, Excitonic and lattice contributions to the charge density wave in  $1T$ -TiSe<sub>2</sub> revealed by a phonon bottleneck, *Phys. Rev. Research* **1**, 023029 (2019).
- [8] K. Sun, S. Sun, C. Zhu, H. Tian, H. Yang and J. Li, Hidden CDW states and insulator-to-metal transition after a pulsed femtosecond laser excitation in layered chalcogenide  $1T$ -TaS<sub>2-x</sub>Se<sub>x</sub>, *Sci. Adv.* **4**, eaas9660 (2018).
- [9] J. A. Wilson, F. J. Di Salvo, and S. Mahajan, Charge-density waves and superlattices in the metallic layered transition metal dichalcogenides, *Adv. Phys.* **24**, 117 (1975).
- [10] L. Perfetti, A. Georges, S. Florens, S. Biermann, S. Mitrovic, H. Berger, Y. Tamm, H. Höchst, and M. Grioni, Spectroscopic Signatures of a Bandwidth-Controlled Mott Transition at the Surface of  $1T$ -TaSe<sub>2</sub>, *Phys. Rev. Lett.* **90**, 166401 (2003).
- [11] K. T. Law and P. A. Lee,  $1T$ -TaS<sub>2</sub> as a quantum spin liquid, *PNAS* **114**, 6996 (2017).
- [12] B. Sipos, A. F. Kusmartseva, A. Akrap, H. Berger, L. Forró and E. Tutiš, From Mott state to superconductivity in  $1T$ -TaS<sub>2</sub>, *Nat. Mater.* **7**, 960 (2008).
- [13] Y. Liu, D. F. Shao, L. J. Li, W. J. Lu, X. D. Zhu, P. Tong, R. C. Xiao, L. S. Ling, C. Y. Xi, L. Pi, H. F. Tian, H. X. Yang, J. Q. Li, W. H. Song, X. B. Zhu, and Y. P. Sun, Nature of charge density waves and superconductivity in  $1T$ -TaSe<sub>2-x</sub>Te<sub>x</sub>, *Phys. Rev. B* **94**, 045131 (2016).
- [14] L. Perfetti, P. A. Loukakos, M. Lisowski, U. Bovensiepen, H. Berger, S. Biermann, P. S. Cornaglia, A. Georges, and M. Wolf, Time Evolution of the Electronic Structure of  $1T$ -TaS<sub>2</sub> through the Insulator-Metal Transition, *Phys. Rev. Lett.* **97**, 067402 (2006).
- [15] L. Perfetti, P. A. Loukakos, M. Lisowski, U. Bovensiepen, M. Wolf, H. Berger, S. Biermann and A. Georges, Femtosecond dynamics of electronic states in the Mott insulator  $1T$ -TaS<sub>2</sub> by time resolved photoelectron spectroscopy, *New. J. Phys.* **10**, 053019 (2008).
- [16] J. C. Petersen, S. Kaiser, N. Dean, A. Simoncig, H. Y. Liu, A. L. Cavalieri, C. Cacho, I. C. E. Turcu, E. Springate, F. Frassetto, L. Poletto, S. S. Dhesi, H. Berger, and A. Cavalleri, Clocking the Melting Transition of Charge and Lattice Order in  $1T$ -TaS<sub>2</sub> with Ultrafast Extreme-Ultraviolet Angle-Resolved Photoemission Spectroscopy, *Phys. Rev. Lett.* **107**, 177402 (2011).
- [17] M. Eichberger, H. Schäfer, M. Krumova, M. Beyer, J. Demsar, H. Berger, G. Moriena, G. Sciaini and R. J. D. Miller, Snapshots of cooperative atomic motions in the optical suppression of charge density waves, *Nature* **468**, 799 (2010).
- [18] L. Stojchevska, I. Vaskivskiy, T. Mertelj, P. Kusar, D. Svetin, S. Brazovskii and D. Mihailovic, Ultrafast switching to a stable hidden quantum state in an electronic crystal, *Science* **11**, 177 (2014).
- [19] C. Sohrt, A. Stange, M. Bauer and K. Rossnagel, How fast can a Peierls-Mott insulator be melted?, *Fara. Dis.* **171**, 243 (2014).
- [20] M. Ligges, I. Avigo, D. Golež, H. U. R. Strand, Y. Beyazit, K. Hanff, F. Diekmann, L. Stojchevska, M. Kalläne, P. Zhou, K. Rossnagel, M. Eckstein, P. Werner, and U. Bovensiepen, Ultrafast Doublon Dynamics in Photoexcited  $1T$ -TaS<sub>2</sub>, *Phys. Rev. Lett.* **120**, 166401 (2018).
- [21] P. Fazekas and E. Tosatti, Charge carrier localization in pure and doped  $1T$ -TaS<sub>2</sub>, *Physica B + C* **99**, 183 (1980).
- [22] T. Ritschel, H. Berger, and J. Geck, Stacking-driven gap formation in layered  $1T$ -TaS<sub>2</sub>, *Phys. Rev. B* **98**, 195134 (2018).
- [23] S.-H. Lee, J. S. Goh, and D. Cho, Origin of the Insulating Phase and First-Order Metal-Insulator Transition in  $1T$ -TaS<sub>2</sub>, *Phys. Rev. Lett.* **122**, 106404 (2019).
- [24] Q. Stahl, M. Kusch, F. Heinsch, G. Garbarino, N. Kretzschmar, K. Hanff, K. Rossnagel, J. Geck, and T. Ritschel, Collapse of layer dimerization in the photo-induced hidden state of  $1T$ -TaS<sub>2</sub>, *Nat. Commun.* **11**, 1247 (2020).
- [25] F. J. Di Salvo, R. G. Maines, J. V. Waszczak, and R. E. Schwall, Preparation and properties of  $1T$ -TaSe<sub>2</sub>, *Solid. State. Comms.* **14**, 497 (1974).
- [26] S. Colonna, F. Ronci, A. Cricenti, L. Perfetti, H. Berger, and M. Grioni, Mott Phase at the Surface of  $1T$ -TaSe<sub>2</sub> Observed by Scanning Tunneling Microscopy, *Phys. Rev. Lett.* **94**, 036405 (2005).
- [27] S. Colonna, F. Ronci, A. Cricenti, L. Perfetti, H. Berger, and M. Grioni, Scanning Tunneling Microscopy Observation of a Mott-Insulator Phase at the  $1T$ -TaSe<sub>2</sub> Surface, *Jpn. J. Appl. Phys.* **45**, 1950 (2006).
- [28] Y. Chen, W. Ruan, M. Wu, S. Tang, H. Ryu, H.-Z. Tsai, R. Lee, S. Kahn, F. Liou, C. Jia, O. R. Albertini, H. Xiong, T. Jia, Z. Liu, J. A. Sobota, A. Y. Liu, J. E. Moore, Z.-X. Shen, S. G. Louie, S.-K. Mo, and M. F. Crommie, Strong correlations and orbital texture in single-layer in  $1T$ -TaSe<sub>2</sub>, *Nat. Phys.* **16**, 218 (2020).
- [29] X. Shi, W. You, Y. Zhang, Z. Tao, P. M. Oppeneer, X. Wu, R. Thomale, K. Rossnagel, M. Bauer, H. Kapteyn and M. Murnane, Ultrafast electron calorimetry uncovers a new long-lived metastable state in  $1T$ -TaSe<sub>2</sub> mediated by mode-selective phonon coupling, *Sci. Adv.* **5**, eaav449 (2019).
- [30] F. Boschini, H. Hedayat, C. Dallera, P. Farinello, C. Manzoni, A. Magrez, H. Berger, G. Cerullo, and E. Carpene, An innovative Yb-based ultrafast deep ultraviolet source for time-resolved photoemission experiments, *Rev. Sci. Inst.* **85**, 123903 (2014).
- [31] C. Manzoni, D. Polli, and G. Cerullo, Two-color pump-probe system broadly tunable over the visible and the near infrared with sub-30 fs temporal resolution, *Rev. Sci. Inst.* **77**, 023103 (2006).
- [32] See Supplemental Material at <http://link.aps.org/> for details of crystal growth, electronic transport measurements, Raman spectroscopy, full-wavevector ARPES, LEED, and further analysis of TR-ARPES data.
- [33] M. Bovet, D. Popović, F. Clerc, C. Koitzsch, U. Probst, E. Bucher, H. Berger, D. Naumović, and P. Aebi, Pseudogapped Fermi surfaces of  $1T$ -TaS<sub>2</sub> and  $1T$ -TaSe<sub>2</sub>: A charge density wave effect, *Phys. Rev. B* **69**, 125117 (2004).
- [34] F. Clerc, M. Bovet, H. Berger, L. Despont, C. Koitzsch, O. Gallus, L. Patthey, M. Shi, J. Krempasky, M. G. Garnier, P. Aebi, Spin-orbit splitting in the valence bands of  $1T$ -TaS<sub>2</sub> and  $1T$ -TaSe<sub>2</sub>, *J. Phys: Condens. Matter* **16**, 3721 (2004).
- [35] P. Aebi, T. Pillo, H. Berger and F. Lévy, On the search for Fermi surface nesting in quasi-2D materials, *J. Electron. Spec. Relat. Phenom.* **117**, 433 (2001).
- [36] P. Knowles, B. Yang, T. Muramatsu, O. Moulding, J. Buhot, C. J. Sayers, E. Da Como, and S. Friedemann, Fermi Surface Reconstruction and Electron Dynamics at the Charge-Density-Wave Transition in TiSe<sub>2</sub>, *Phys.*

- 489 [Rev. Lett. \*\*124\*\*, 167602 \(2020\).](#)
- 490 [37] M. P. Seah and W. A. Dench, Quantitative electron spec- 501  
491 troscopy of surfaces: A standard data base for electron 502  
492 inelastic mean free paths in solids, [Surf. Interface Anal. \*\*1\*\*, 2 \(1979\).](#) 503  
493  
494 [38] S. Ji, O. Grånäs, K. Rossnagel, and J. Weissenrieder, 504  
495 Transient three-dimensional structural dynamics in 1 *T*- 505  
496 TaSe<sub>2</sub>, [Phys. Rev. B. \*\*101\*\*, 094303 \(2020\).](#) 506  
497 [39] J. Demsar, L. Forro, H. Berger and D. Mihailovic, Fem- 507  
498 tosecond snapshots of gap-forming charge-density-wave 508  
499 correlations in quasi-two-dimensional dichalcogenides 509  
500 1 *T*-TaS<sub>2</sub> and 2 *H*-TaSe<sub>2</sub>, [Phys. Rev. B. \*\*66\*\*, 041101\(R\) 510](#)  
511  
512  
513  
514  
515  
516  
517  
518  
519  
520  
521  
522  
523  
524  
525  
526  
527  
528  
529  
530  
531  
532  
533  
534  
535  
536  
537  
538  
539  
540  
541  
542  
543  
544  
545  
546  
547  
548  
549  
550  
551  
552  
553  
554  
555  
556  
557  
558  
559  
560  
561  
562  
563  
564  
565  
566  
567  
568  
569  
570  
571  
572  
573  
574  
575  
576  
577  
578  
579  
580  
581  
582  
583  
584  
585  
586  
587  
588  
589  
590  
591  
592  
593  
594  
595  
596  
597  
598  
599  
600  
601  
602  
603  
604  
605  
606  
607  
608  
609  
610  
611  
612  
613  
614  
615  
616  
617  
618  
619  
620  
621  
622  
623  
624  
625  
626  
627  
628  
629  
630  
631  
632  
633  
634  
635  
636  
637  
638  
639  
640  
641  
642  
643  
644  
645  
646  
647  
648  
649  
650  
651  
652  
653  
654  
655  
656  
657  
658  
659  
660  
661  
662  
663  
664  
665  
666  
667  
668  
669  
670  
671  
672  
673  
674  
675  
676  
677  
678  
679  
680  
681  
682  
683  
684  
685  
686  
687  
688  
689  
690  
691  
692  
693  
694  
695  
696  
697  
698  
699  
700  
701  
702  
703  
704  
705  
706  
707  
708  
709  
710  
711  
712  
713  
714  
715  
716  
717  
718  
719  
720  
721  
722  
723  
724  
725  
726  
727  
728  
729  
730  
731  
732  
733  
734  
735  
736  
737  
738  
739  
740  
741  
742  
743  
744  
745  
746  
747  
748  
749  
750  
751  
752  
753  
754  
755  
756  
757  
758  
759  
760  
761  
762  
763  
764  
765  
766  
767  
768  
769  
770  
771  
772  
773  
774  
775  
776  
777  
778  
779  
780  
781  
782  
783  
784  
785  
786  
787  
788  
789  
790  
791  
792  
793  
794  
795  
796  
797  
798  
799  
800  
801  
802  
803  
804  
805  
806  
807  
808  
809  
810  
811  
812  
813  
814  
815  
816  
817  
818  
819  
820  
821  
822  
823  
824  
825  
826  
827  
828  
829  
830  
831  
832  
833  
834  
835  
836  
837  
838  
839  
840  
841  
842  
843  
844  
845  
846  
847  
848  
849  
850  
851  
852  
853  
854  
855  
856  
857  
858  
859  
860  
861  
862  
863  
864  
865  
866  
867  
868  
869  
870  
871  
872  
873  
874  
875  
876  
877  
878  
879  
880  
881  
882  
883  
884  
885  
886  
887  
888  
889  
890  
891  
892  
893  
894  
895  
896  
897  
898  
899  
900  
901  
902  
903  
904  
905  
906  
907  
908  
909  
910  
911  
912  
913  
914  
915  
916  
917  
918  
919  
920  
921  
922  
923  
924  
925  
926  
927  
928  
929  
930  
931  
932  
933  
934  
935  
936  
937  
938  
939  
940  
941  
942  
943  
944  
945  
946  
947  
948  
949  
950  
951  
952  
953  
954  
955  
956  
957  
958  
959  
960  
961  
962  
963  
964  
965  
966  
967  
968  
969  
970  
971  
972  
973  
974  
975  
976  
977  
978  
979  
980  
981  
982  
983  
984  
985  
986  
987  
988  
989  
990  
991  
992  
993  
994  
995  
996  
997  
998  
999  
1000
- [40] J. E. Smith, Jr. J. C. Tsang, and M. W. Shafer, Raman spectra of several layer compounds with charge density waves, [Solid. State. Comms. \*\*19\*\*, 283 \(1976\).](#)
- [41] J. C. Tsang, J. E. Smith Jr., M. Shafer and S. F. Meyer, Raman spectroscopy of the charge-density-wave state in 1 *T*- and -2 *H*-TaSe<sub>2</sub>, [Phys. Rev. B. \*\*16\*\*, 4239 \(1977\).](#)
- [42] S. Uchida and S. Sugai, Infrared and Raman studies on commensurate CDW states in transition metal dichalcogenides, [Physica. B+C \*\*105\*\*, 393 \(1981\).](#)
- [43] S. Sugai, K. Murase, S. Uchida, and S. Tanaka, Comparison of the soft modes in tantalum dichalcogenides, [Physica. B+C \*\*105\*\*, 405 \(1981\).](#)